Gastroenterology 2022;162:1690–1704

PUFA-Induced Metabolic Enteritis as a Fuel for Crohn's Disease

Julian Schwärzler,[1,*] **Lisa Mayr**,[1,*] **Arnau Vich Vila**,[2,*] Felix Grabherr,[1] Lukas Niederreiter,[1] Maureen Philipp,[1] Christoph Grander,[1] Moritz Meyer,[1] Almina Jukic,[1] Simone Tröger,[1] Barbara Enrich,[1] Nicole Przysiecki,[1] Markus Tschurtschenthaler,[3,4] Felix Sommer,[5] Irmgard Kronberger,[6] Jakob Koch,[7] Richard Hilbe,[8] Michael W. Hess,[9] Georg Oberhuber,[10] Susanne Sprung,[11] Qitao Ran,[12] Robert Koch,[1] Maria Effenberger,[1] Nicole C. Kaneider,[13] Verena Wieser,[14] Markus A. Keller,[7] Rinse K. Weersma,[2] Konrad Aden,[5] Philip Rosenstiel,[5] Richard S. Blumberg,[15] Arthur Kaser,[13] Herbert Tilg,[1] and Timon E. Adolph[1]

[1]Department of Internal Medicine I, Gastroenterology, Hepatology, Endocrinology, and Metabolism, Medical University of Innsbruck, Innsbruck, Austria; [2]Department of Gastroenterology and Hepatology, University of Groningen and Groningen University Medical Center, Groningen, The Netherlands; [3]Institute for Experimental Cancer Therapy, Center for Translational Cancer Research (TranslaTUM), Klinikum rechts der Isar, Technical University of Munich, Munich, Germany; [4]Department of Internal Medicine II, Klinikum rechts der Isar, Technical University of Munich, Munich, Germany; [5]Institute of Clinical Molecular Biology, Christian Albrecht University Kiel and Schleswig-Holstein University Hospital, Kiel, Germany; [6]Department of Visceral, Transplant, and Thoracic Surgery, Medical University of Innsbruck, Innsbruck, Austria; [7]Institute of Human Genetics, Medical University of Innsbruck, Innsbruck, Austria; [8]Department of Internal Medicine II, Infectious Diseases, Immunology, Rheumatology, Pneumology, Medical University of Innsbruck, Innsbruck, Austria: [9]Institute of Histology and Embryology, Medical University of Innsbruck, Innsbruck, Austria; [10]INNPATH, Innsbruck Medical University Hospital, Innsbruck, Austria; [11]Department of Pathology, Medical University of Innsbruck, Innsbruck, Austria; [12]Department of Cell Systems and Anatomy, UT Health San Antonio, San Antonio, Texas; [13]Division of Gastroenterology and Hepatology, Department of Medicine, Addenbrooke's Hospital, University of Cambridge, Cambridge, United Kingdom; [14]Department of Obstetrics and Gynecology, Medical University of Innsbruck, Innsbruck, Austria; and [15]Gastroenterology Division, Department of Medicine, Brigham and Women's Hospital, Harvard Medical School, Boston, Massachusetts

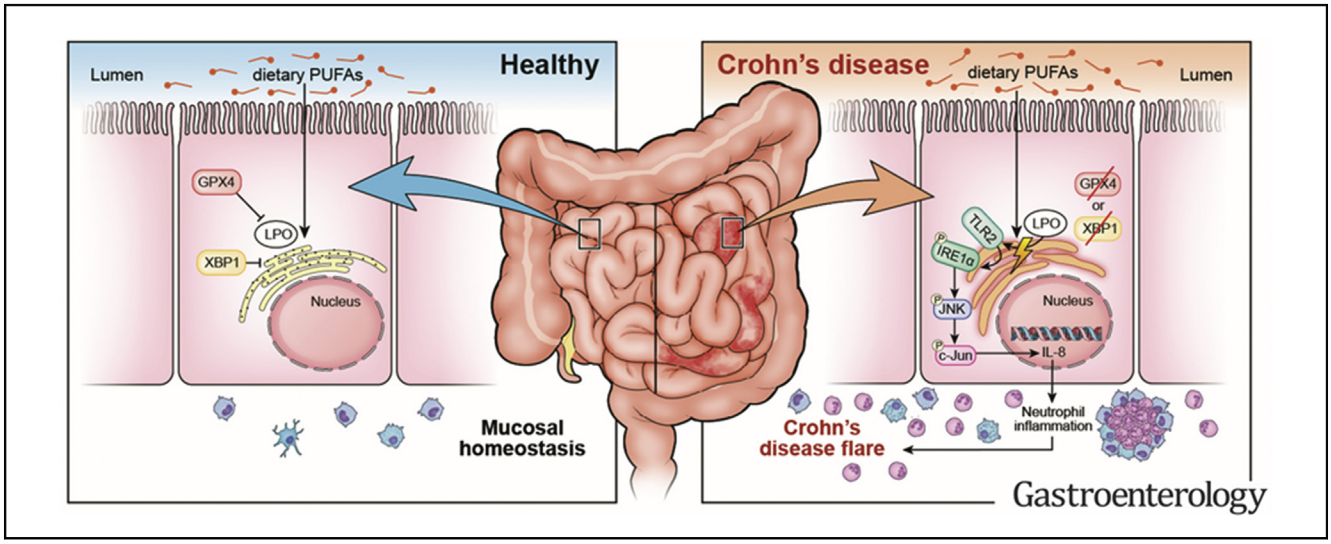

See editorial on page 1590.

BACKGROUND & AIMS: Crohn's disease (CD) globally emerges with Westernization of lifestyle and nutritional habits. However, a specific dietary constituent that comprehensively evokes gut inflammation in human inflammatory bowel diseases remains elusive. We aimed to delineate how increased intake of polyunsaturated fatty acids (PUFAs) in a Western diet, known to impart risk for developing CD, affects gut inflammation and disease course. We hypothesized that the unfolded protein response and antioxidative activity of glutathione peroxidase 4 (GPX4), which are compromised in human CD epithelium, compensates for metabolic perturbation evoked by dietary PUFAs. **METHODS:** We phenotyped and mechanistically dissected enteritis evoked by a PUFA-enriched Western diet in 2 mouse models exhibiting endoplasmic reticulum (ER) stress consequent to intestinal epithelial cell (IEC)–specific deletion of *X-box binding protein 1* (*Xbp1*) or *Gpx4*. We translated the findings to human CD epithelial organoids and correlated PUFA intake, as estimated by a dietary questionnaire or stool metabolomics, with clinical disease course in 2 independent CD cohorts. **RESULTS:** PUFA excess in a Western diet potently induced ER stress, driving enteritis in $Xbp1^{-/-IEC}$ and

Gpx4$^{+/-IEC}$ mice. ω-3 and ω-6 PUFAs activated the epithelial endoplasmic reticulum sensor inositol-requiring enzyme 1α (IRE1α) by toll-like receptor 2 (TLR2) sensing of oxidation-specific epitopes. TLR2-controlled IRE1α activity governed PUFA-induced chemokine production and enteritis. In active human CD, ω-3 and ω-6 PUFAs instigated epithelial chemokine expression, and patients displayed a compatible inflammatory stress signature in the serum. Estimated PUFA intake correlated with clinical and biochemical disease activity in a cohort of 160 CD patients, which was similarly demonstrable in an independent metabolomic stool analysis from 199 CD patients. **CONCLUSIONS:** We provide evidence for the concept of PUFA-induced metabolic gut inflammation which may worsen the course of human CD. Our findings provide a basis for targeted nutritional therapy.

Keywords: Glutathione Peroxidase 4; X-Box–Binding Protein 1; ω-3 Polyunsaturated Fatty Acids; ω-6 Polyunsaturated Fatty Acids; Endoplasmic Reticulum Stress.

Westernization of life style and dietary habits is paralleled by an accelerating incidence of inflammatory bowel diseases, such as Crohn's disease (CD), especially in newly industrialized countries.[1] It is conceived that the increasing incidence of inflammatory bowel diseases is largely explained by environmental factors such as Westernization of diet, which is partially characterized by an increased consumption of long-chain fatty acids.[2–4] For example, population-based estimates of Western dietary habits (in the USA in the 20th century) and dietary monitoring programs indicated an increased intake of ω-6 polyunsaturated fatty acids (PUFAs) contained in meat, eggs, and oils.[5–7] In consideration of documented beneficial effects of ω-3 PUFAs on, for example, cardiovascular risk, the United States Food and Drug Administration approved ω-3 PUFA supplementation of food (eg, enrichment of animal feed) in 2014,[8] which was similarly suggested by the European Food Safety Authority. In this concept, which is based on widely documented antiinflammatory actions of ω-3 PUFAs (while ω-6 PUFAs fuel inflammatory metabolites[7,9]), general recommendations suggest dietary enrichment with ω-3 PUFAs while avoiding excessive intake of ω-6 PUFAs. However, the direct impact of PUFAs on gut health is poorly defined. A systematic analysis of epidemiologic studies comprising large prospective cohorts indicated that total PUFA intake imparts a risk for developing CD.[10–12] Moreover, the EPIC trials (EPANOVA in Crohn's Disease; NCT00613197 and NCT00074542) indicated that ω-3 PUFA supplementation was ineffective in maintaining remission in CD,[13] and a recent Cochrane meta-analysis indicated that PUFA supplementation worsened gastrointestinal symptoms in patients with CD.[14] In turn, elemental diets that partly reduce PUFA intake effectively induced and maintained remission.[15,16] Collectively, these studies suggested that dietary PUFAs confer risk for developing CD and possibly affect the course of established CD. However, the mechanisms that control a detrimental inflammatory response in the intestine on exposure to a Western diet (WD) and specifically PUFAs remain enigmatic.

WHAT YOU NEED TO KNOW

BACKGROUND AND CONTEXT

Environmental factors and specifically the diet directly affect gut microbial communities and immune responses. A dietary constituent that comprehensively triggers gut inflammation in patients with inflammatory bowel disease remains elusive.

NEW FINDINGS

We demonstrate experimental evidence that an excess of dietary polyunsaturated fatty acids in a Western diet triggers metabolic inflammation in the gut, which may deteriorate the course of Crohn's disease.

LIMITATIONS

Targeted nutritional clinical trials are warranted to confirm the detrimental role of dietary polyunsaturated fatty acids for patients with Crohn's disease.

IMPACT

Our study provides a basis for targeted nutritional therapies in patients with Crohn's disease.

Glutathione peroxidase 4 (GPX4) is a selenoenzyme that protects against lipid peroxidation, the generation of oxidation-specific epitopes, and cell death termed ferroptosis,[17] which can be pharmacologically exploited to treat human malignancies.[18,19] More specifically, GPX4 limits oxidation of arachidonylated phosphatidylethanolamines (a class of membrane phospholipids), which is fueled by dietary PUFAs.[20] We recently modeled impaired intestinal epithelial GPX4 activity, a feature of human CD, by generating mice that specifically deleted 1 *Gpx4* allele in intestinal epithelial cells (IECs), referred to as *Gpx4*$^{+/-IEC}$ mice[21]. *Gpx4*$^{+/-IEC}$ mice exposed to a PUFA-enriched WD (supplemented with 10% fish oil containing ω-3 and ω-6 PUFAs) displayed small intestinal neutrophilic inflammation.[21] Impaired GPX4 activity in IECs allowed interleukin-6 (IL6) and chemokine (C-X-C motif) ligand 1 (CXCL1) expression on dietary PUFA exposure, which was, however, not paralleled with ferroptosis. As such, a mechanism for how PUFAs induce gut inflammation has remained elusive, the concept of metabolic gut inflammation has been poorly explored, and implications for CD patients remain undetermined.

Metabolic inflammation, prototypically observed in obesity, refers to an inflammatory state that is evoked by dietary excess of nutrients such as long-chain fatty acids.[22,23]

*** Authors share co-first authorship.**

Abbreviations used in this paper: **CD, Crohn's disease; CXCL1, chemokine (C-X-C motif) ligand 1; GPX4, glutathione peroxidase 4; ER, endoplasmic reticulum; IEC, intestinal epithelial cell; IL, interleukin; IRE1α, inositol-requiring enzyme 1α; JNK, c-Jun N-terminal kinase; PUFA, polyunsaturated fatty acid; TLR2, Toll-like receptor 2; TNF, tumor necrosis factor; WD, Western diet; WT, wild-type; XBP1, X-box–binding protein 1.**

Most current article

0016-5085
https://doi.org/10.1053/j.gastro.2022.01.004

Metabolic inflammation is orchestrated by metabolically active cells and the immune system in adipose, liver, and muscle tissue.[22,23] For example, long-chain fatty acids induce the unfolded protein response in the liver, which allows cellular adaptation to endoplasmic reticulum (ER) stress.[24] ER stress triggers activation of ER sensors such as inositol-requiring enzyme 1α (IRE1α) and subsequent unconventional splicing of *X-box binding protein 1* (*Xbp1*) to resolve accumulation of un- or misfolded proteins.[25] In contrast, unresolved ER stress drives a range of inflammatory diseases. In obesity, ER stress and specifically IRE1α serve as a rheostat for inflammation in metabolically active tissues.[26,27] Likewise, unresolved ER stress is implicated in the pathogenesis of inflammatory bowel disease.[28] For example, unresolved ER stress due to deletion of *Xbp1* specifically in IECs of mice instigates inflammation in the small intestine that is governed by IRE1α.[29,30] Based on these studies, we hypothesized that dietary PUFAs trigger ER stress, fueling enteritis in CD. By analyzing transgenic mouse models, human CD organoids, and 2 independent patient cohorts, we identified dietary PUFAs as a fuel for epithelial ER stress, reporting here a mechanism of PUFA-induced gut inflammation and linking PUFA intake in CD patients with poor disease course.

Materials and Methods

See the Supplementary Materials and Methods.

Results

A Western Diet Enriched With ω-3 and ω-6 PUFAs Evokes Epithelial ER Stress, Chemokine Production, and Enteritis in $Xbp1^{-/-IEC}$ Mice

In a first step, we assessed a role for intestinal epithelial ER stress in PUFA-induced gut inflammation. We enriched a WD with 10% fish oil (containing ω-3 and ω-6 PUFAs in a 7:1 ratio), referred to as PUFA-enriched WD (Supplementary Table 1), and exposed $Xbp1^{-/-IEC}$ mice (displaying epithelial ER stress[29]) and wild-type (WT) littermates to this diet for 3 months. A standard WD or a low-fat diet served as a control (Supplementary Table 1). $Xbp1^{-/-IEC}$ mice displayed severe enteritis after exposure to a PUFA-enriched WD compared with WT mice or $Xbp1^{-/-IEC}$ mice on a low-fat diet or standard WD, which was characterized by loss of gut architecture and submucosal infiltration of mono- and polymorphonuclear cells (Figure 1*A–C* and Supplementary Figure 1*A–C*). Indeed, neutrophil granulocytes and macrophages (but not other innate or adaptive immune cells) accumulated in the mucosa of $Xbp1^{-/-IEC}$ mice compared with WT controls, as assessed by means of flow cytometry phenotyping (Figure 1*D* and *E* and Supplementary Figure 1*D–G*). The abundance of specialized intestinal epithelial cells (such as Paneth cells or Goblet cells) in $Xbp1^{-/-IEC}$ mice was unaffected by a PUFA-enriched WD (Supplementary Figure 2*A–D*), and epithelial cell death was not a feature of PUFA-induced enteritis in $Xbp1^{-/-IEC}$ mice (Supplementary Figure 2*E* and *F*). Similarly, the colon of $Xbp1^{-/-IEC}$ mice was morphologically comparable to that of WT mice on a PUFA-enriched WD (Supplementary Figure 2*G* and *H*). PUFA-induced enteritis was characterized by increased epithelial ER stress (Figure 1*F* and Supplementary Figure 2*I* and *J*), activation of c-Jun N-terminal kinases (JNKs) (Figure 1*F* and Supplementary Figure 2*K* and *L*), epithelial release of the IL-8 homolog CXCL1 and IL-6 (Figure 1*G* and Supplementary Figure 2*M*), systemic low-grade inflammation (Figure 1*H–J* and Supplementary Figure 3*A* and *B*), and impaired body weight gain (Figure 1*K*). In a reductionist system using small-intestinal MODE-K epithelial cells, dietary ω-3 and ω-6 PUFAs (exemplified with stearidonic acid and arachidonic acid) evoked ER stress and IRE1α activation, as well as chemokine production specifically in IECs with impaired *Xbp1* expression (Supplementary Figure 3*C–F*). Collectively, these data indicated that dietary PUFAs deteriorated epithelial ER stress, chemokine production, and enteritis, which are limited by XBP1.

GPX4 Restricts Epithelial ER Stress Evoked by ω-3 and ω-6 PUFAs, Which Drives Enteritis in Mice

In a next step, we explored whether epithelial ER stress is a driver of PUFA-induced gut inflammation in $Gpx4^{+/-IEC}$ mice that develop enteritis (affecting ~30%–50% of the lower small intestine), but not colitis, characterized by granuloma-like lesions involving neutrophil granulocytes and $F4/80^{+}$ macrophages after exposure to a PUFA-enriched WD for 3 months (Supplementary Figure 4*A–E*).[21] ω-3 and ω-6 PUFAs potently instigated epithelial ER stress (Supplementary Figure 4*F–H*), IRE1α activation (Figure 2*A* and *B*), JNK signaling (Figure 2*C* and Supplementary Figure 4*I*), and production of CXCL1 and IL-6 in *siGpx4* IECs (Supplementary Figure 4*J–L*). Likewise, $Gpx4^{+/-IEC}$ mice displayed signs of epithelial ER stress as well as IRE1α and JNK activation after exposure to a PUFA-enriched WD (Figure 2*D–G* and Supplementary Figure 5*A–F*). Enteritis was characterized by mucosal CXCL1 and IL-6 production (Supplementary Figure 5*G* and *H*), accumulation of neutrophil granulocytes (Supplementary Figure 5*I* and *J*), and systemic low-grade inflammation (Supplementary Figure 5*K–N*). Abundance of specialized epithelial cells (such as Paneth cells) was similar between $Gpx4^{+/-IEC}$ and WT mice exposed to a PUFA-enriched WD (Supplementary Figure 6*A–D*).[21] In line with a critical role for epithelial ER stress, treatment by the chaperone tauro-urso-deoxycholic acid (TUDCA)[31] protected against PUFA-induced enteritis in $Gpx4^{+/-IEC}$ mice (Figure 2*H* and *I*), and prevented PUFA-induced epithelial JNK activation and chemokine production (Figure 2*J* and *K* and Supplementary Figure 6*E*). In a genetic approach, we assessed whether the ER sensor IRE1α, a critical regulator of JNK activity,[32] governs PUFA-induced chemokine production and enteritis in the context of impaired GPX4 activity. Indeed, co-silencing of *Ern1* (encoding IRE1α) blunted PUFA-induced JNK activation (Supplementary Figure 6*F* and *G*) and abrogated PUFA-induced chemokine production (Figure 2*L* and Supplementary Figure 6*H*), similar to co-silencing of *Jnk1/2* (Figure 2*M* and Supplementary Figure 6*I–K*). Deletion of *Ern1*

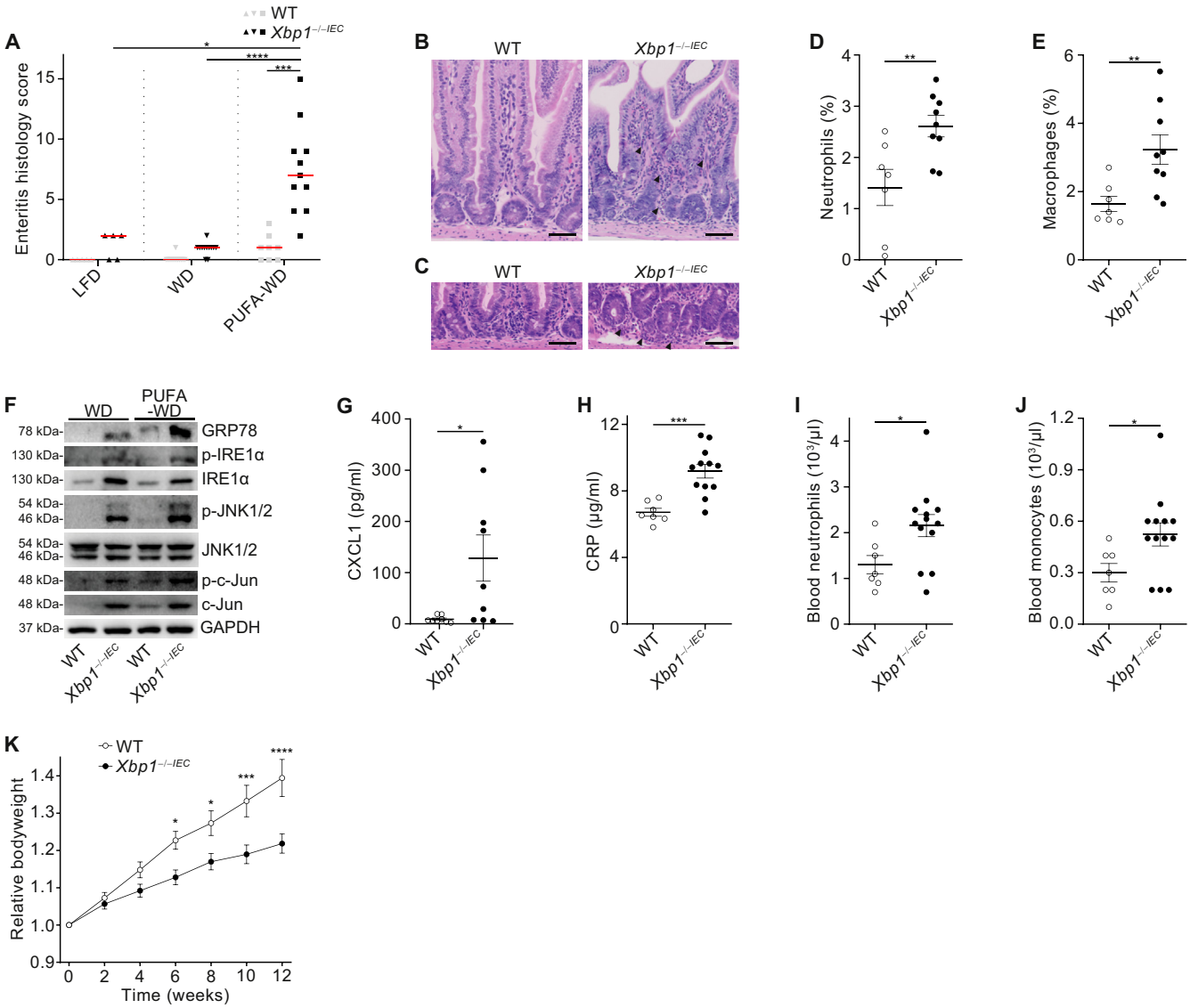

Figure 1. ω-3 and ω-6 PUFAs evoke epithelial ER stress fueling chemokine production and enteritis in *Xbp1*$^{-/-IEC}$ mice. (*A*) Histology score for WT and *Xbp1*$^{-/-IEC}$ mice after exposure to a LFD, WD, or PUFA-enriched WD (PUFA-WD) (n $\geq$ 5). Medians indicated by *red lines*. (*B, C*) Representative H&E images of the small intestine of WT and *Xbp1*$^{-/-IEC}$ mice exposed to a PUFA-WD. Note severe mucosal inflammation in *Xbp1*$^{-/-IEC}$ mice with infiltration of neutrophil granulocytes in the mucosa and submucosa (*arrows*). Scale bar, 50 μm. (*D, E*) Quantification of (*D*) Ly6G-expressing neutrophil granulocytes and (*E*) MERTK-expressing macrophages in the mucosa of WT and *Xbp1*$^{-/-IEC}$ mice exposed to a PUFA-WD (n = 7 and 9). (*F*) Representative immunoblot from small-intestinal epithelial scrapings of WT and *Xbp1*$^{-/-IEC}$ mice exposed to a PUFA-WD compared with standard WD (n $\geq$ 3 mice). (*G, H*) Quantification of (*G*) CXCL1 and (*H*) CRP in the supernate of cultured primary IECs from WT and *Xbp1*$^{-/-IEC}$ mice exposed to a PUFA-WD (n $\geq$ 7). (*I, J*) Quantification of (*I*) neutrophil granulocytes and (*J*) monocytes in blood counts of WT and *Xbp1*$^{-/-IEC}$ mice fed a PUFA-WD for 3 months (n = 7/13). (*K*) Weight course of WT and *Xbp1*$^{-/-IEC}$ mice fed a PUFA-WD relative to the initial body weight of each experiment animal (n = 16 and 17). CRP, C-reactive protein; CXCL1, C-X-C motif chemokine ligand 1; H&E, hematoxylin and eosin; IEC, intestinal epithelial cell; IRE1α, inositol-requiring enzyme 1α; JNK, c-Jun N-terminal kinase; LFD, low-fat diet; PUFA, polyunsaturated fatty acid; WD, Western diet; WT, wild-type; Xbp1, *X-box–binding protein 1*.

specifically in IECs from *Gpx4*$^{+/-IEC}$ mice (ie, *Ern1*$^{-/-IEC}$/*Gpx4*$^{+/-IEC}$ mice) protected against enteritis induced by a PUFA-enriched WD, compared with *Gpx4*$^{+/-IEC}$ mice (Figure 2*N* and *O* and Supplementary Figure 6*L*). Likewise, pharmacologic inhibition of JNK signaling by SP600125[33] protected *Gpx4*$^{+/-IEC}$ mice against enteritis evoked by a PUFA-enriched WD (Figure 2*P* and Figure S6*M* and *N*), and SP600125 abolished PUFA-induced epithelial chemokine production (Supplementary Figure 6*O* and *P*). Moreover, functional blockade of the CXCL1 receptor CXCR1/2 by pepducin x-1/2pal-i1[34] protected against PUFA-induced enteritis in *Gpx4*$^{+/-IEC}$ mice (Figure 2*P* and Supplementary Figure 6*M* and *N*). Collectively, these data unambiguously demonstrated that PUFA-induced epithelial ER stress drives enteritis in *Gpx4*$^{+/-IEC}$ mice, and that the ER sensor IRE1α governs PUFA-induced chemokine production and enteritis.

Next, we corroborated which dietary ω-3 and ω-6 PUFAs trigger enteritis. We exposed *Gpx4*$^{+/-IEC}$ and WT littermates to a WD for 3 months and then orally inoculated ω-3 α-linolenic acid (C18:3), ω-3 eicosapentaenoic acid (C20:5), ω-3 docosahexaenoic acid (C22:6), or ω-6 arachidonic acid (C20:4) once daily for 2 weeks, and the monounsaturated

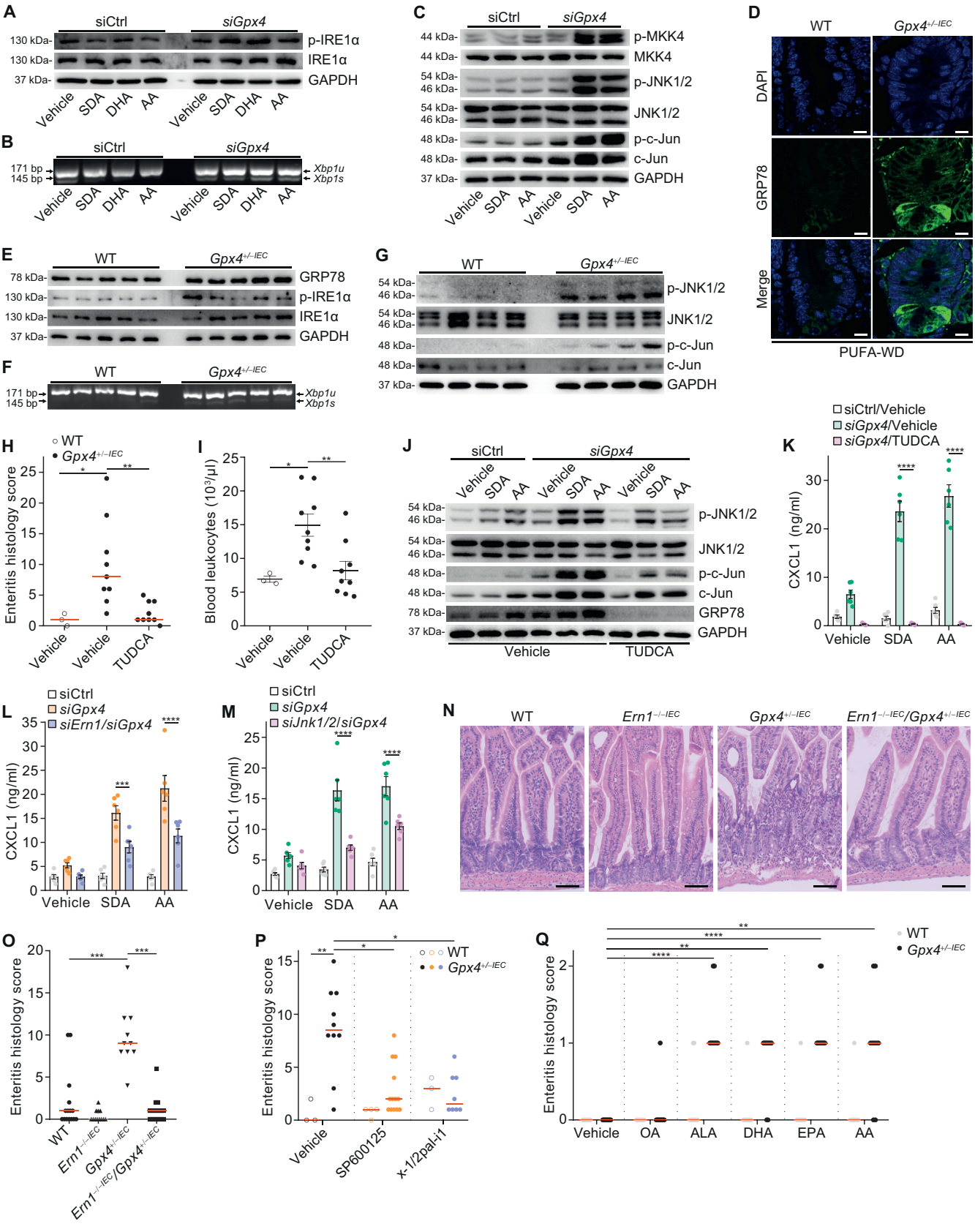

fatty acid oleic acid (C18:1) or vehicle gavage served as a control. Notably, ω-3 PUFAs triggered neutrophilic infiltration in *Gpx4*$^{+/-IEC}$ mice, but not in WT mice, to an extent similar to the ω-6 PUFA arachidonic acid (Figure 2*Q* and Supplementary Figure 7*A* and *B*). Moreover, intestinal inflammation was demonstrable in *Gpx4*$^{+/-IEC}$ mice exposed to a 3-month WD enriched with 10% soybean oil (containing ω-6 linoleic acid, ω-3 α-linolenic acid, and ω-3 stearidonic acid in a 1:8 ratio of ω-3 to ω-6) (Figure S7*C* and *D* and Supplementary Table 1). PUFA-induced enteritis was demonstrable 2 weeks (but not 3 months) after switching back to a chow diet (Supplementary Figure 7*E*–*G*). These data indicated that both ω-3 and ω-6 PUFAs instigate intestinal inflammation in WD-fed *Gpx4*$^{+/-IEC}$ mice.

TLR2 Translates PUFA-Induced Epithelial Lipid Peroxidation Into ER Stress and Enteritis

In a next step, we explored how dietary PUFAs evoke epithelial ER stress. GPX4 is a selenoenzyme known to limit lipid peroxidation,[17] which led us to hypothesize that oxidative phospholipid perturbation fuels epithelial ER stress and chemokine production in our model.[21] Indeed, ω-3 and ω-6 PUFAs induced accumulation of oxidized phospholipids and oxidation-specific epitopes in *siGpx4* IECs (Figure 3*A* and *B*), and lipid peroxidation localized to the ER (Figure 3*C* and Supplementary Figure 8*A*). We did not note altered phospholipid membrane composition as determined by means of liquid chromatography/dual mass spectrometry in *siGpx4* IECs compared with siCtrl (Supplementary Figure 8*B*–*D*). To genetically corroborate that GPX4-restricted lipid peroxidation and the generation of oxidation-specific epitopes instigate ER stress, we generated IECs that expressed a mutant GPX4 variant encompassing cysteine instead of a selenocysteine at its catalytic site (GPX4^{cys}) (Supplementary Figure 9*A*), which is expected to impair enzymatic GPX4 activity.[35] Indeed, GPX4^{cys} IECs displayed increased lipid peroxidation (Supplementary Figure 9*B*), whereas GPX4 expression was retained compared with WT IECs (Figure S9*C*). Notably, GPX4^{cys} IECs displayed signs of IRE1α activation (Figure 3*D*) and responded with JNK activation and CXCL1 production on PUFA stimulation (Supplementary Figure 9*D*–*F*). Likewise, biochemical induction of lipid peroxidation by oxidized phosphatidylcholine instigated IRE1α activation and CXCL1 production in *siGpx4* IECs (Figure 3*E* and Supplementary Figure 9*G*–*I*). In line with this, exposure of IECs to oxidation-specific epitopes, such as 4-HNE or MDA, evoked IRE1α activation, JNK signaling, and chemokine production (Figure 3*F*–*H* and Supplementary Figure 9*J* and *K*). In turn, induction of ER stress by chemical means potently impaired GPX4 activity and induced lipid peroxidation in IECs (Figure 3*I* and *J* and Supplementary Figure 9*L*), which we similarly observed in IECs from *Xbp1*$^{-/-IEC}$ mice (Figure 3K and Supplementary Figure 9*M*). Moreover, a PUFA-enriched WD potently induced intestinal epithelial lipid peroxidation and accumulation of oxidation-specific epitopes in *Xbp1*$^{-/-IEC}$ mice and in *Gpx4*$^{+/-IEC}$ mice (Figure 3*L* and *M* and Supplementary Figure 9*N*–*Q*). These data demonstrated that PUFAs induce epithelial lipid peroxidation and accumulation of oxidation-specific epitopes in IECs, which instigates ER stress and IRE1α activation restricted by *Xbp1* and *Gpx4*.

In a next step, we hypothesized that oxidation-specific epitopes instigated intestinal epithelial ER stress by pattern recognition receptor signaling.[36,37] We noted that oxidized phospholipids and oxidation-specific epitopes such as 4-HNE and MDA induced toll-like receptor 2 (TLR2) activation in a reporter cell line (Figure 3*N*), and that TLR2 partially localized to the ER in IECs (Supplementary

Figure 2. PUFA-induced enteritis in *Gpx4*$^{+/-IEC}$ mice is governed by ER stress and IRE1α activation. (*A, B*) Representative images of IRE1α activation in siCtrl and *siGpx4* IECs after stimulation with ω-3 PUFA (SDA, DHA) or ω-6 PUFA (AA) for 24 hours, as assessed by (*A*) immunoblot and (*B*) *Xbp1* splicing assay (n = 3). (*C*) Representative immunoblot of JNK signaling in siCtrl and *siGpx4* IECs after stimulation with SDA or AA for 24 hours (n = 3). (*D*) Representative confocal images of GRP78 (*green*) in crypts of WT and *Gpx4*$^{+/-IEC}$ mice fed a PUFA-WD for 3 months. DAPI (*blue*) indicates nucleus. Scale bar, 10 μm. Note that the same images are also shown in Supplementary Figure 5*A* with the respective LFD control samples. (*E, F*) Representative images of IRE1α activation indicated by (*E*) immunoblot and (*F*) *Xbp1* splicing assay in small-intestinal epithelial scrapings of WT and *Gpx4*$^{+/-IEC}$ mice exposed to a PUFA-WD (n $\geq$ 5 mice per genotype). (*G*) Representative immunoblot of JNK signaling of small-intestinal epithelial scrapings from WT and *Gpx4*$^{+/-IEC}$ mice exposed to a PUFA-WD (n = 4 mice per genotype). (*H*) Histology score for WT and *Gpx4*$^{+/-IEC}$ mice exposed to a PUFA-WD and treatment with TUDCA or vehicle (n = 3, 9, and 9). (*I*) Quantification of blood leukocytes (blood count) of WT and *Gpx4*$^{+/-IEC}$ mice treated with TUDCA or vehicle for the last 14 days of exposure to a PUFA-WD for 3 months (n = 3, 9, and 9). (*J*) Representative immunoblot of JNK1/2 and c-Jun phosphorylation in siCtrl and *siGpx4* IECs stimulated with ω-3 PUFA (SDA) or ω-6 PUFA (AA) and treated with or without TUDCA for 24 hours. Representative of n = 3 independent experiments. (*K*) Quantification of CXCL1 in the supernate of siCtrl and *siGpx4* IECs stimulated with SDA or AA and treated with TUDCA for 24 hours (n = 6). (*L*) Quantification of CXCL1 in the supernate of siCtrl and *siGpx4* IECs with or without co-silencing of *Ern1* (encoding IRE1α) after stimulation with SDA or AA for 24 hours (n = 6). (*M*) Quantification of CXCL1 in the supernate of siCtrl and *siGpx4* IECs with or without co-silencing *Jnk1/2* and after stimulation with SDA or AA for 24 hours (n = 3). (*N, O*) Representative (*N*) H&E images (scale bar, 100 μm) and (*O*) histology scores of indicated genotypes after exposure to a PUFA-WD (n = 15, 12, 10, and 18). (*P*) Histology score of WT and *Gpx4*$^{+/-IEC}$ mice fed a PUFA-WD and treated with the JNK inhibitor SP600125 or the CXCR1/2 inhibitory pepducin x-1/2pal-i1 (or vehicle) (n = 3, 10, 4, 13, 3, and 8). (*Q*) Histology scores of WT and *Gpx4*$^{+/-IEC}$ mice exposed to WD and daily oral gavage of ω-3 PUFA ALA, DHA, or EPA or the ω-6 PUFA AA as compared with vehicle or the monounsaturated fatty acid OA during the last 2 weeks of the experiment (n $\geq$ 8). AA, arachidonic acid; ALA, α-linolenic acid; DHA, docosahexaenoic acid; EPA, eicosapentaenoic acid; ER, endoplasmic reticulum; *Gpx4, glutathione peroxidase 4*; SDA, stearidonic acid; TUDCA, tauro-urso-deoxycholic acid; other abbreviations as in Figure 1.

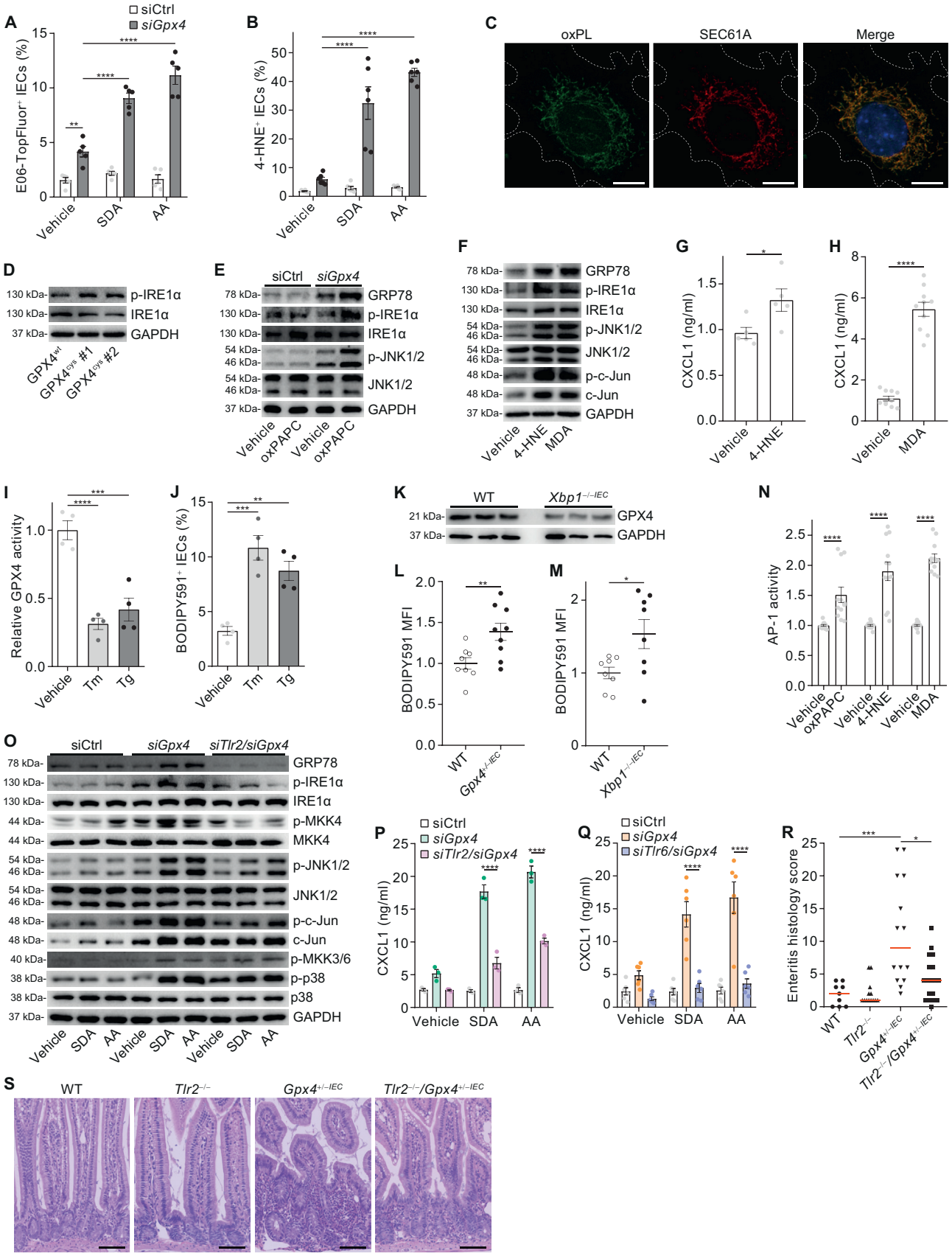

BASIC AND TRANSLATIONAL AT

Figure 10*A*). Co-silencing of *Tlr2* prevented PUFA-induced IRE1α activation and signs of ER stress in *siGpx4* IECs (Figure 3*O* and Supplementary Figure 10*B*). In line with this, co-silencing of *Tlr2* prevented PUFA-induced JNK activation (Figure 3*O*) and chemokine production (Figure 3*P* and Supplementary Figure 10*C*) in *siGpx4* IECs, while TLR2 did not control PUFA-induced lipid peroxidation (Supplementary Figure 10*D*). Likewise, co-silencing of the TLR2 co-receptor *Tlr6*[38] blunted PUFA-induced chemokine production in *siGpx4* IECs (Figure 3*Q* and Figure 10*E* and *F*). In contrast, co-silencing of other toll-like receptors (ie, *Tlr3*, *Tlr4*, *Tlr7*, *Tlr8*, and *Tlr9*) or the fatty acid receptor *Cd36*[36] did not affect PUFA-induced chemokine production in *siGpx4* IECs (Supplementary Figure 10*G–N*). Notably, co-deletion of *Tlr2* in $Gpx4^{+/-IEC}$ mice protected against PUFA-induced enteritis (Figure 3*R* and *S* and Supplementary Figure 10*O*). These data indicated that dietary ω-3 and ω-6 PUFAs trigger epithelial accumulation of oxidation-specific epitopes, instigating TLR2-mediated IRE1α activation, chemokine production, and enteritis, which is restricted by GPX4.

Antibiotic Depletion of the Commensal Microbiota Ameliorates PUFA-Induced Enteritis

Because dietary challenges and specifically PUFAs are critical regulators of the commensal gut microbiota,[39] we analyzed fecal microbiota composition by means of 16S rDNA amplicon sequencing of co-housed WT and $Gpx4^{+/-IEC}$ littermates that had been exposed to our dietary regimens (ie, chow control diet, low-fat diet, WD, or PUFA-enriched WD) for 3 months. We noted a reduction in α-diversity in both WT and $Gpx4^{+/-IEC}$ mice exposed to a PUFA-enriched WD compared with a regular chow diet (according to Shannon diversity and number of operational taxonomic units) (Figure S11*A* and *B*), as similarly reported for mice and humans exposed to a Western-style diet.[40,41] Importantly, at the β-diversity level (ie, diversity between groups, measured by unweighted UniFrac), each dietary condition exhibited a distinct fecal microbiota composition, which was independent from the respective genotype (Figure 4*A*). More specifically, the fecal microbiota composition of PUFA-enriched WD–fed WT mice was indistinguishable from that of $Gpx4^{+/-IEC}$ mice (Figure 4*B–D*). Furthermore, we assessed whether the presence of a commensal microbiota contributed to PUFA-induced enteritis. To do so, we exposed $Gpx4^{+/-IEC}$ mice (and WT littermates) to a PUFA-enriched WD for 3 months and treated them with vancomycin and metronidazole in drinking water for the last 2 weeks. Notably, antibiotic treatment ameliorated PUFA-induced enteritis in $Gpx4^{+/-IEC}$ mice (Figure 4*E* and *F*). These data indicated that a PUFA-enriched WD did not alter bacterial composition in $Gpx4^{+/-IEC}$ mice (compared with WT), while eradication of the commensal gut microbiota ameliorated PUFA-induced enteritis.

PUFA Exposure Triggers Epithelial Cytokine Expression in Human CD, and Intake Correlates With Active Disease Course

We previously reported that IECs from CD patients exhibit impaired small-intestinal epithelial GPX4 activity,[21] which is paralleled by signs of epithelial ER stress.[28,29] To demonstrate that PUFAs elicit an inflammatory response from IECs in CD, we generated human small intestinal epithelial organoids from 6 healthy control subjects and 6

Figure 3. TLR2 translates epithelial lipid peroxidation into ER stress and enteritis. (*A*, *B*) Quantification of oxidation-specific epitopes in siCtrl or *siGpx4* IECs after stimulation with ω-3 PUFA (SDA) or ω-6 PUFA (AA) for 24 hours, as assessed by means of flow cytometry of (*A*) E06-TopFluor$^+$ or (*B*) 4-HNE$^+$ IECs (n = 5 and 6). (*C*) Representative confocal images of oxidized phospholipids (oxPL; *green*) indicated by E06-TopFluor and the endoplasmic reticulum transporter SEC61 (*red*) in *siGpx4* IECs after stimulation with ω-6 PUFA (AA) for 24 hours. Spearman's rank correlation coefficient = 0.60 between green and red localization. DAPI (*blue*) indicates nucleus. *Dashed line* indicates outer plasma membrane. Scale bar, 10 μm. n = 3 individual experiments. (*D*) Representative immunoblot from two GPX4^{cys} clones and WT IECs indicating IRE1α activation (n = 3). (*E*) Representative immunoblot indicating IRE1α activation and JNK signaling in siCtrl and *siGpx4* IECs after stimulation with oxPAPC or vehicle for 24 hours (n = 3). (*F*) Representative immunoblot from WT IECs indicating IRE1α activation and JNK signaling after stimulation with 4-HNE or MDA (or vehicle) for 24 hours (n = 3). (*G*, *H*) Quantification of CXCL1 in the supernate from WT IECs after stimulation with (*G*) 4-HNE or (*H*) MDA (or vehicle) for 24 hours (n = 5 and 10). (*I*) Relative GPX4 enzymatic activity of Tm- or Tg-stimulated IECs for 24 hours compared with vehicle (n = 4). (*J*) Quantification of lipid peroxidation in Tm- or Tg-stimulated IECs compared with vehicle, as assessed by flow cytometry of BODIPY581/591 C11$^+$ (n = 4). (*K*) Representative GPX4 immunoblot of IEC scrapings from WT and $Xbp1^{-/-IEC}$ mice exposed to a chow diet (n = 3 for each genotype). (*L*) Quantification of lipid peroxidation according to BODIPY581/591 C11$^+$ MFI as assessed by flow cytometry of IEC isolates of WT and $Gpx4^{+/-IEC}$ mice exposed to a PUFA-WD for 3 months (n = 8 and 9). (*M*) Quantification of lipid peroxidation by BODIPY581/591 C11$^+$ MFI in IEC isolates of WT and $Xbp1^{-/-IEC}$ mice exposed to a PUFA-WD for 3 months, as assessed by flow cytometry (n = 8). (*N*) Relative activity of the transcription factor AP-1 in a colorimetric TLR2 reporter cell line (indicative for TLR2 activation) after stimulation with oxPAPC or related by-products 4-HNE or MDA for 16 hours (n = 4). (*O*) Representative immunoblot of siCtrl or *siGpx4* IECs with or without co-silencing of *Tlr2* after stimulation with SDA or AA for 24 hours. Note that *Tlr2* co-silencing abolished PUFA-induced IRE1α and JNK activation in *siGpx4* IECs (n = 3). (*P*, *Q*) Quantification of CXCL1 in the supernate of siCtrl and *siGpx4* IECs with or without co-silencing of (*P*) *Tlr2* or (*Q*) *Tlr6* and after stimulation with SDA or AA for 24 hours (n $\geq$ 3). (*R*) Histology scores of indicated genotypes shown in (*S*) that were exposed to a PUFA-WD (n = 9, 13, 14, and 18). Medians indicated by *red lines*. (*S*) Representative H&E images of the small intestine from indicated genotypes exposed to a PUFA-WD. Note mucosal inflammation in $Gpx4^{+/-IEC}$ mice and protection against enteritis in $Gpx4^{+/-IEC}$ mice co-deleted for *Tlr2*. Scale bar, 50 μm. 4-HNE, 4-hydroxynonenal; MDA, malondialdehyde; MFI, median fluorescent intensity; oxPAPC, oxidized 1-palmitoyl-2-arachidonoyl-sn-glycero-3-phosphocholine; Tg, thapsigargin; Tm, tunicamycin; other abbreviations as in Figures 1 and 2.

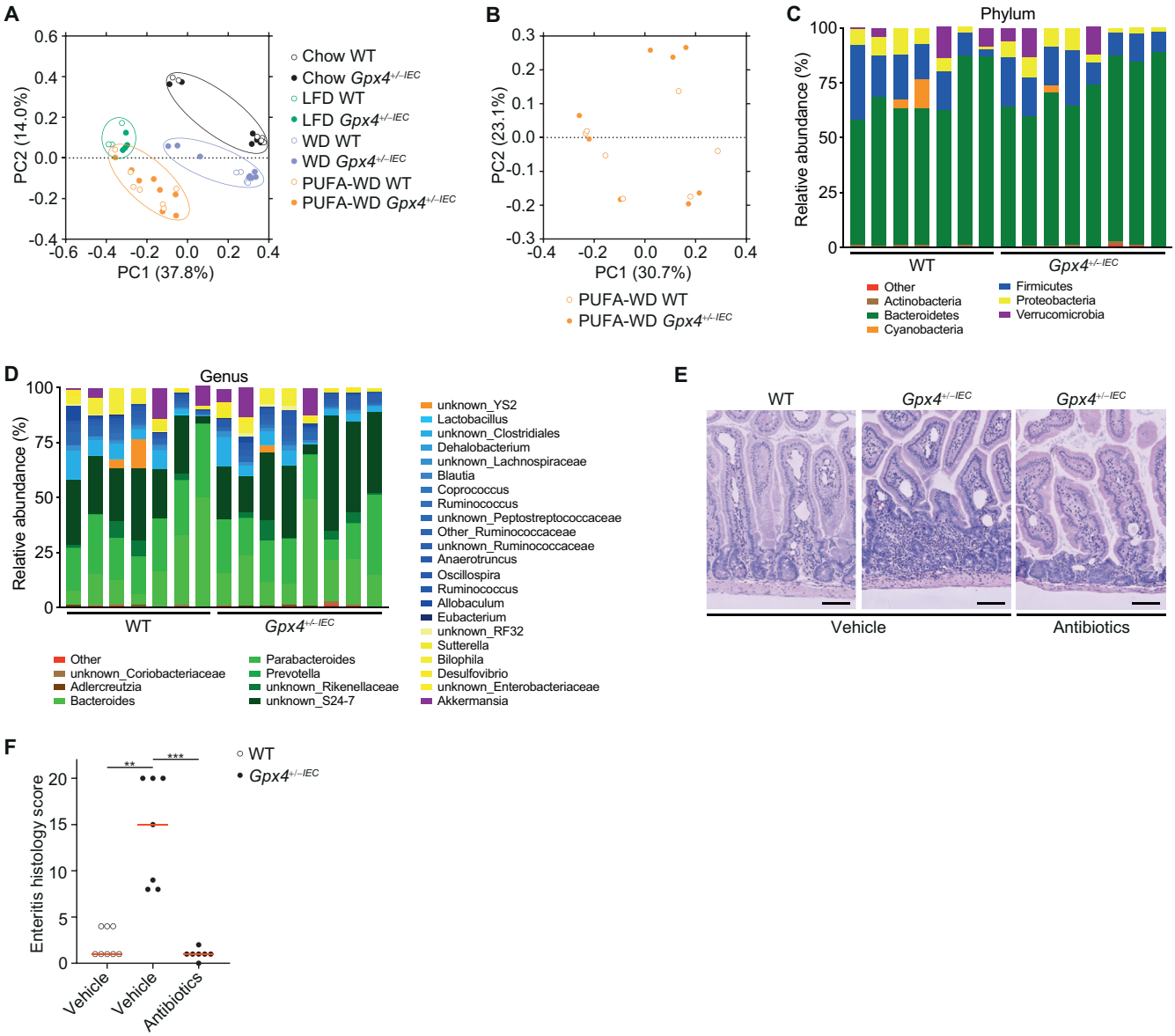

Figure 4. Antibiotic depletion of the commensal gut microbiota ameliorates PUFA-induced enteritis in *Gpx4*$^{+/-IEC}$ mice. (*A*) β-Diversity indicated by PC analysis of indicated dietary conditions and co-housed genotypes (based on unweighted UniFrac analysis) (n $\geq$ 3 for each genotype). (*B*) β-Diversity of co-housed WT and *Gpx4*$^{+/-IEC}$ mice exposed to a PUFA-WD indicated by PC analysis. Statistical significance was assessed by means of permutational multivariate analysis of variance. (*C*) Relative abundance of indicated taxa at phylum level of co-housed WT and *Gpx4*$^{+/-IEC}$ mice on a PUFA-WD (n = 8 for each genotype). (*D*) Relative abundance of indicated taxa at genus level of indicated co-housed genotypes fed a PUFA-WD (n = 7 and 8). (*E*) Representative H&E images of the small intestine from WT and *Gpx4*$^{+/-IEC}$ mice exposed to a PUFA-WD treated with antibiotics. Scale bar, 50 μm. (*F*) Histology scores of indicated genotypes shown in (*E*) that were exposed to a PUFA-WD and treated with antibiotics (n = 8, 7 and 7). Medians indicated by *red lines*. PC, principal component; other abbreviations as in Figures 1 and 2.

patients with active CD, who underwent ileocecal resection (Supplementary Table 2). Notably, ω-3 and ω-6 PUFAs triggered *IL8* and tumor necrosis factor (*TNF*α) expression only in CD organoids with impaired GPX4 expression (Figure 5*A* and *B* and Supplementary Figure 12*A*), which was associated with signs of lipid peroxidation (Figure 5*C* and Supplementary Figure 12*B*). *IL6* expression was barely detectable in CD organoids with or without PUFA stimulation (data not shown). Our findings in mice suggested that PUFAs induced an inflammatory signature involving IL-8, ER stress, and accumulation of oxidation-specific epitopes. To approximate the number of CD patients with such an inflammatory signature and to establish a direct relation between PUFA intake and the course of CD, we investigated a cohort that was recruited in our outpatient clinic from 2013 to 2016 and followed by standard clinical practice for 5.36 $\pm$ 1.42 years. At study inclusion, we used a questionnaire (Supplementary Table 3)[42] to retrieve dietary information, and we collected serum samples from 62 CD patients with active disease and 98 quiescent CD patients (in clinical remission). Forty-nine volunteers who displayed no history or clinical or biochemical evidence of

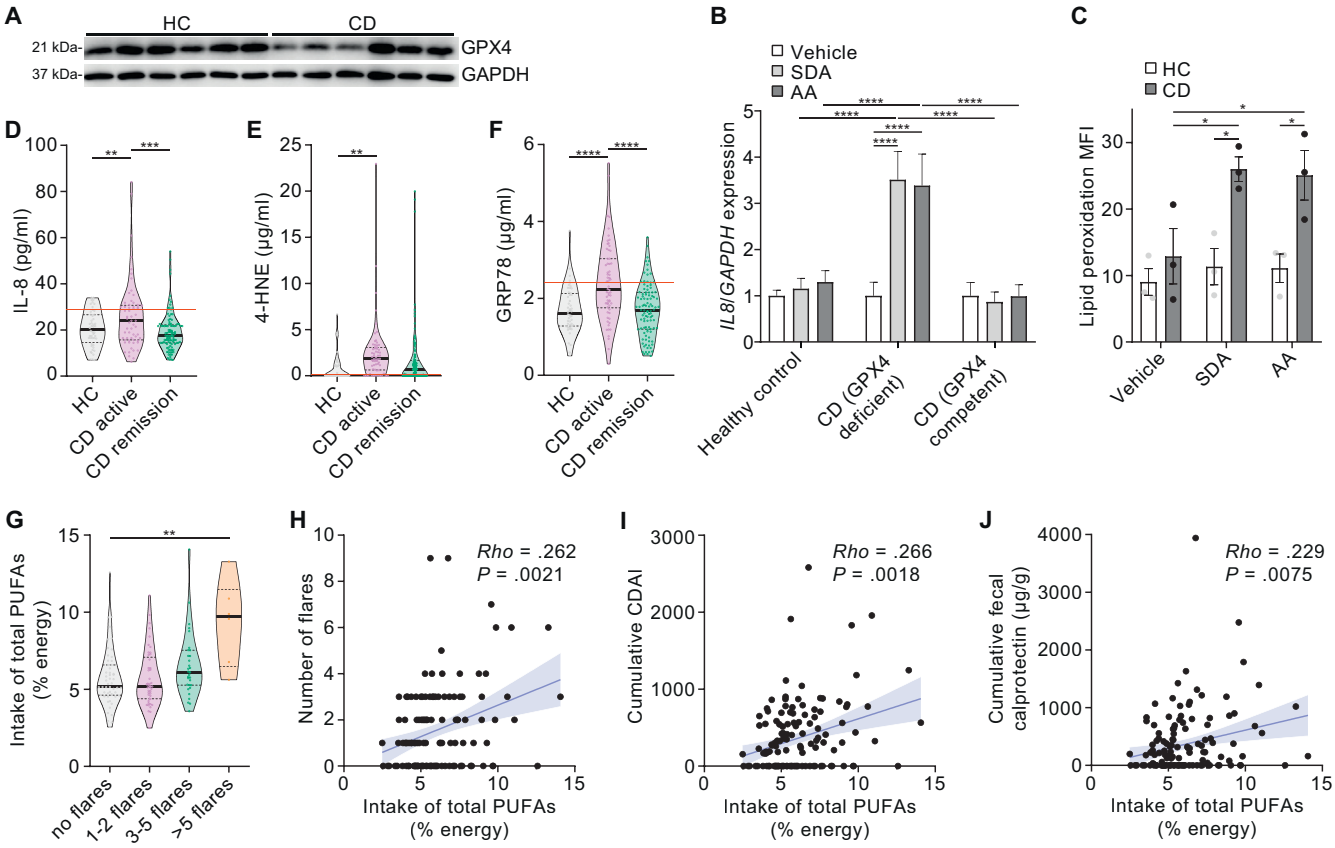

Figure 5. PUFA exposure triggers epithelial cytokine expression in human CD, and PUFA intake correlates with active disease course. (*A*) GPX4 immunoblot of cultured small intestinal epithelial organoids from 6 HC subjects and 6 active CD patients that underwent ileocecal resection. GAPDH served as loading control. (*B*) Quantification of interleukin-8 (*IL8*) expression of small intestinal epithelial organoids from CD patients and HC subjects in a monolayer model after SDA or AA stimulation for 24 hours. Expression is stratified according to GPX4 activity compared with HC subjects (*A*) and normalized to *GAPDH* (n ≥ 3 per group). (*C*) Quantification of lipid peroxidation as determined by Click-iT assay immunofluorescence intensity of small-intestinal epithelial organoids from CD patients after SDA or AA stimulation for 24 hours, compared with HC subjects (n = 3). (*D–F*) Quantification of (*D*) IL-8, (*E*) 4-HNE, and (*F*) glucose-regulated protein 78 (GRP78) in the serum of HC subjects and patients with active or quiescent CD (n = 49, 62, and 98). The *red line* denotes the disease-discriminating threshold determined with the use of the Youden index (Supplementary Figure 13*A–C*). Medians indicated by *solid black lines*. (*G*) Relationship between estimated relative PUFA intake per week (based on a dietary questionnaire) and the number of CD flares during the observational period (n = 52, 45, 32, and 6). Medians indicated by *solid black lines*. (*H–J*) Correlation of estimated relative PUFA intake per week (based on a dietary questionnaire) and (*H*) number of flares, (*I*) cumulative Crohn's Disease Activity Index (CDAI; ie, the sum of CDAI >150), and (*J*) cumulative fecal calprotectin in µg/g during the observational period in CD patients (n = 135), depicted by linear regression (*shadows* depict 95% confidence interval). CD, Crohn's disease; HC, healthy control; other abbreviations as in Figures 1–3.

gastrointestinal disease served as healthy control subjects (clinical characteristics summarized in Supplementary Table 4). Indeed, we noted an inflammatory serum signature in active CD comprising IL-8, accumulation of oxidation-specific epitopes, and signs of ER stress (Figure 5*D–F* and Supplementary Figure 12*C*), which correlated with clinical and biochemical disease activity (Supplementary Figure 12*D–K*) and which was reversed by immunomodulatory treatment with anti-TNF antibodies (Supplementary Figure 12*L–O* and Supplementary Table 5). We assessed a disease-discriminating cutoff by means of the Youden index for each surrogate (ie, IL-8, 4-HNE, and GRP78) (Supplementary Figure 13*A–C*), as detailed in the Supplementary Materials and Methods, to then approximate the proportion of patients with this inflammatory signature. Notably, the inflammatory signature (≥2 surrogates above the disease-discriminating cutoff) was demonstrable in ∼60% of active CD patients (Supplementary Table 6) and was associated with ileal (rather than isolated colonic) disease (Supplementary Figure 13*D*).

Finally, we related estimated dietary PUFA intake (determined by the food frequency questionnaire) to the disease course indicated by the cumulative Crohn's Disease Activity Index (CDAI) and the cumulative fecal calprotectin concentration (ie, the sum of each flare) during the observational period (Supplementary Figure 13*E* and *F* and Supplementary Table 7). We chose that approach so as to depict the disease burden during the observational period rather than disease burden at a single time point. Medical

therapy before study inclusion was similar between patients that experienced disease flares (≥2) during the observational period and those patients who did not experience disease flares (Supplementary Table 8). In contrast, CD patients who experienced flares during the observational period were subjected to a change in medical therapy more often (Supplementary Table 9). Importantly, estimated PUFA intake directly correlated with the number of CD flares, cumulative CDAI, and cumulative fecal calprotectin concentration in the observational period (Figure 5*G–J* and Supplementary Figure 13*G–I*). Collectively, these data indicated that active CD patients exhibited a systemic inflammatory signature that can be triggered by dietary PUFAs, and that dietary PUFA intake correlates with a poor disease course.

Fecal PUFA Abundance Directly Correlates With CD Activity

To corroborate these findings in an independent cohort, we analyzed 199 CD patients (55 active and 144 inactive CD patients at the time of sampling visit) in the Dutch 1000IBD cohort (clinical characteristics presented in Supplementary Table 10; patient stratification shown in Supplementary Figure 14*A*.[43] In this cohort, we took advantage of specific fecal ω-3 and ω-6 PUFA quantification by means of untargeted metabolomics, an unbiased approach that allows detection of dietary PUFA intake in a WD in human stool.[44,45] CD patients in remission, similarly to active CD patients, displayed increased total PUFA abundance in stool compared with healthy control subjects (Figure 6*A*), which can be explained by increased ω-3 as well as ω-6 PUFA abundance (Supplementary Figure 14*B–G*), and which appeared to be unrelated to the CD-associated *GPX4* variant rs2024092 (Supplementary Figure 14*H–N*).[46] To assess the relation between PUFA abundance in stool and clinical disease activity, we used multivariate linear regression, while taking into account potential confounders such as patient-related variables (ie, age, sex, body mass index, number of intestinal resections, disease location, and daily bowel movements) and technical confounders (ie, batch, amount of input fecal material, and storage time). By doing so, we noted that total fecal PUFA concentration, and specifically fecal ω-3 and ω-6 PUFA abundance, directly correlated with the number of disease flares (Figure 6*B–D* and Supplementary Figure 14*O–R*) and cumulative clinical CD activity (Figure 6*E–G*, Supplementary Figure 14*S–V*, and Supplementary Table 11). Collectively, our findings indicate that dietary PUFA intake correlates with a poor course of human CD.

Discussion

The WD and an excess of dietary PUFAs are suspected of putting humans at risk for developing CD.[8,10] In already established CD, an elemental diet is able to potently induce and maintain remission of disease[15,16,47] and thus serves as first-line therapy in pediatric CD.[48] The therapeutic efficacy of an elemental diet appears to depend on reduced availability of long-chain fatty acids, but not of other nutrients.[15,49] Similarly, the efficacy of an exclusion diet in CD was attributable to the exclusion of pork, beef, eggs, and milk, potent sources of PUFAs.[50] These studies suggest that dietary modulation affects the course of CD. However, elemental diets are unpalatable and poorly tolerated, which has resulted in impaired adherence and high discontinuation rates (~40%) in adult clinical trials.[48] Although studies suggest that dietary long-chain fatty acids may be detrimental to CD patients,[10,12,15] no CD-specific evidence-based diet can be recommended to prevent or treat adult CD.[51,52] This may be partially explained by the facts that no dietary constituent has been identified as a trigger of CD today and that mechanisms of dietary lipid–induced mucosal immune responses in the intestine remain poorly understood. Here, we report how dietary PUFAs disrupt gut health by perturbation of epithelial stress responses, which we translate to human CD.

Long-chain fatty acids are taken up in IECs of the small intestine, re-esterified into complex lipid molecules, and assembled into lipoproteins at the ER (eg, chylomicrons) to allow uptake into the circulation through the lymphatic system.[53] Moreover, long-chain fatty acids, and specifically PUFAs, are incorporated in cellular membranes at the ER and targeted for oxidation, which is specifically restricted by GPX4.[20] GPX4-restricted lipid peroxidation mediates ferroptosis,[17] while mechanisms of inflammatory tissue injury, for example, in mice that lack *Gpx4* specifically in the brain[54] or skin,[55] are largely unexplored. Here, we report that intestinal epithelial GPX4 protects against ER perturbation evoked by a dietary PUFA challenge. In IECs with impaired GPX4 activity, ω-3 and ω-6 PUFAs evoke lipid peroxidation and generation of oxidation-specific epitopes that instigated ER stress and IRE1α activation via TLR2. Consequently, PUFA-induced ER stress and IRE1α-mediated JNK activation drive gut inflammation in $Gpx4^{+/-IEC}$ mice, which phenocopies aspects of human CD (ie, patchy submucosal infiltration of immune cells, formation of granuloma-like neutrophilic lesions, and lymphatic vessel dilation)[56] (Supplementary Figure 15). The critical role of ER stress in this model is corroborated by studies in $Xbp1^{-/-IEC}$ mice, demonstrating that XBP1-restricted epithelial ER stress deteriorated on exposure to a PUFA-enriched WD, which was paralleled by severe enteritis. We acknowledge that the reported phenotype in these genetically susceptible mice exposed to a 3-month PUFA-enriched WD depicts an acute (rather than chronic) inflammatory response in the gut and lacks evidence of villous atrophy, a histopathologic sign of severe enteritis in CD. This reported mechanism is compelling, because previous studies demonstrated that ER stress–mediated IRE1α activity serves as an inflammatory signaling hub in 3 mouse models that spontaneously resemble human CD, ie, in $Xbp1^{-/-IEC}$, aged $Atg16l1^{-/-IEC}$, and $Atg16l1^{-/-IEC}$/$Xbp1^{-/-IEC}$ mice,[29,30,57] thus supporting the notion that dietary factors and genetic susceptibility (involving common *ATG16L1* and/or *GPX4* variants and rare *XBP1* variants) culminate in CD by a converging mechanism.[4,46]

In a translational approach, we demonstrate that dietary ω-3 and ω-6 PUFAs trigger *IL8* and *TNFα* expression of IECs

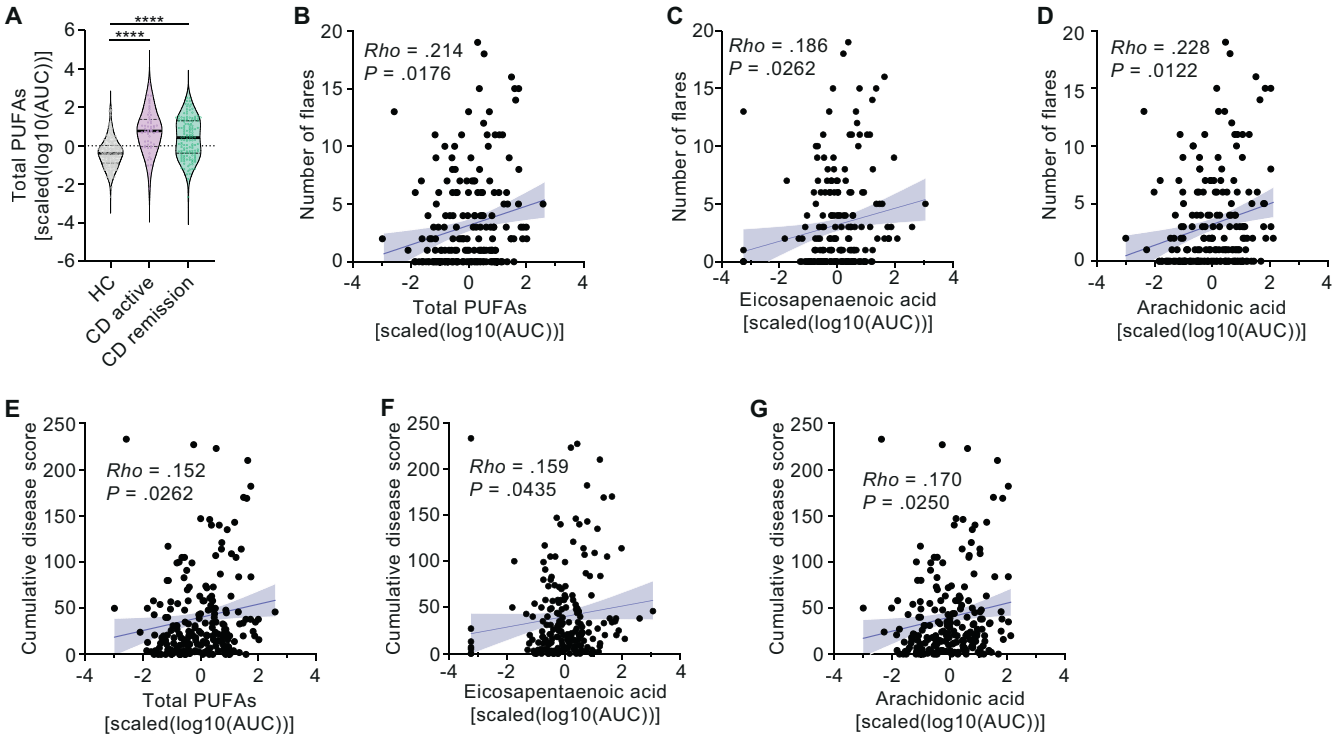

Figure 6. Fecal PUFA abundance correlates with CD activity. (*A*) Fecal total PUFA abundance in active (n = 55) and inactive (n = 144) CD patients compared with non–inflammatory bowel disease population control subjects (n = 255), as indicated by untargeted metabolomic analysis. Total PUFA abundance was estimated by summing chromatographic peaks for AA, EPA, SDA, DPA, and DHA (see Materials and Methods). Violin plots with median and interquartile range. Active disease was defined as a Harvey-Bradshaw Index ≥5. (*B–D*) Correlation of relative (*B*) total PUFA abundance, (*C*) EPA, and (*D*) AA in the feces of CD patients and the number of CD flares during the observational period (n = 199), depicted by linear regression (*shadows* depict 95% confidence interval). (*E–G*) Correlation of relative (*E*) total PUFA abundance, (*F*) EPA, and (*G*) AA in the feces of CD patients with the cumulative disease activity index (ie, the sum of flares defined by Harvey-Bradshaw Index) during the observational period (n = 199), depicted by linear regression (shadows depict 95% confidence interval). AUC, area under the receiver operating characteristic curve; other abbreviations as in Figures 1, 2, and 5.

derived from CD patients with impaired GPX4 expression. A systemic inflammatory signature (comprising IL-8, oxidation-specific epitopes, or surrogates for ER stress) can be detected in ∼60% of active CD patients, suggesting that our findings are relevant to human disease. In line with this, estimated dietary PUFA intake or fecal ω-3 and ω-6 PUFA concentration in stool directly correlated with long-term CD activity as indicated by number of CD flares and clinical disease indices in 2 independent CD cohorts. Moreover, biochemical disease activity (ie, cumulative fecal calprotectin concentration) correlated with estimated PUFA intake.

Several limitations of these clinical observations are noteworthy. The food frequency questionnaire used to estimate PUFA intake in our CD cohort is prone to bias (eg, recall bias) and does not allow highly accurate resolution of nutrient intake. These are aspects of any questionnaire-based assessment,[58] which led us to study an independent cohort with the use of an independent technique (ie, stool metabolomics) to detect intake of long-chain fatty acids in individuals exposed to a WD.[45] The untargeted metabolomic approach in that independent cohort also indicated that PUFA intake directly correlates with a poor clinical course of CD. We acknowledge that our assessment of disease activity in both cohorts involved clinical and biochemical parameters but not endoscopy readouts. However, recent studies indicate that fecal calprotectin concentration reasonably correlates with endoscopic disease activity.[59]

Altogether, our study demonstrates experimental and translational evidence for a detrimental role of ω-3 and ω-6 PUFAs on mammalian gut health, as they trigger an inflammatory response in genetically susceptible epithelium in some patients with CD. Our study sheds light on the failure of previous ω-3 PUFA supplementation trials that did not allow maintenance of remission in CD,[13,60] and indicates the need to identify patients that are unable to cope with an excess of dietary PUFAs. Our study may also provide an understanding of the risk association between PUFA intake and gut inflammation in CD[10] and may explain some efficacy of exclusive enteral nutrition in active CD.[16] Furthermore, our data suggest that a habitual human diet specifically designed to reduce excessive ω-3 and ω-6 PUFA intake may prevent or ameliorate the course of CD. Serum assays could help to identify patients with a systemic inflammatory signature as identified here, to guide patient-tailored dietary advice or medical therapy, a concept that warrants controlled clinical trials.

Supplementary Material

Note: To access the supplementary material accompanying this article, visit the online version of Gastroenterology at www.gastrojournal.org, and at https://doi.org/10.1053/j.gastro.2022.01.004.

References

1. Ng SC, Shi HY, Hamidi N, et al. Worldwide incidence and prevalence of inflammatory bowel disease in the 21st century: a systematic review of population-based studies. Lancet 2018;390:2769–2778.
2. d'Haens GR, Geboes K, Peeters M, et al. Early lesions of recurrent Crohn's disease caused by infusion of intestinal contents in excluded ileum. Gastroenterology 1998; 114:262–267.
3. Rutgeerts P, Goboes K, Peeters M, et al. Effect of faecal stream diversion on recurrence of Crohn's disease in the neoterminal ileum. Lancet 1991;338:771–774.
4. Roda G, Chien Ng S, Kotze PG, et al. Crohn's disease. Nat Rev Dis Primers 2020;6:22.
5. Blasbalg TL, Hibbeln JR, Ramsden CE, et al. Changes in consumption of omega-3 and omega-6 fatty acids in the United States during the 20th century. Am J Clin Nutr 2011;93:950–962.
6. Sugihara K, Morhardt TL, Kamada N. The role of dietary nutrients in inflammatory bowel disease. Front Immunol 2018;9:3183.
7. Khalili H, Chan SSM, Lochhead P, et al. The role of diet in the aetiopathogenesis of inflammatory bowel disease. Nat Rev Gastroenterol Hepatol 2018;15:525–535.
8. Ganesan B, Brothersen C, McMahon DJ. Fortification of foods with omega-3 polyunsaturated fatty acids. Crit Rev Food Sci Nutr 2014;54:98–114.
9. Donowitz M. Arachidonic acid metabolites and their role in inflammatory bowel disease. An update requiring addition of a pathway. Gastroenterology 1985;88:580–587.
10. Hou JK, Abraham B, El-Serag H. Dietary intake and risk of developing inflammatory bowel disease: a systematic review of the literature. Am J Gastroenterol 2011; 106:563–573.
11. Lee D, Albenberg L, Compher C, et al. Diet in the pathogenesis and treatment of inflammatory bowel diseases. Gastroenterology 2015;148:1087–1106.
12. Costea I, Mack DR, Lemaitre RN, et al. Interactions between the dietary polyunsaturated fatty acid ratio and genetic factors determine susceptibility to pediatric Crohn's disease. Gastroenterology 2014;146:929–931.
13. Feagan BG, Sandborn WJ, Mittmann U, et al. Omega-3 free fatty acids for the maintenance of remission in Crohn disease: the EPIC randomized controlled trials. JAMA 2008;299:1690–1697.
14. Lev-Tzion R, Griffiths AM, Leder O, et al. Omega 3 fatty acids (fish oil) for maintenance of remission in Crohn's disease. Cochrane Database Syst Rev 2014;2: CD006320.
15. Narula N, Dhillon A, Zhang D, et al. Enteral nutritional therapy for induction of remission in Crohn's disease. Cochrane Database Syst Rev 2018;4:CD000542.
16. Riordan AM, Hunter JO, Cowan RE, et al. Treatment of active Crohn's disease by exclusion diet: East Anglian multicentre controlled trial. Lancet 1993;342:1131–1134.
17. Stockwell BR, Friedmann Angeli JP, Bayir H, et al. Ferroptosis: a regulated cell death nexus linking metabolism, redox biology, and disease. Cell 2017; 171:273–285.
18. Viswanathan VS, Ryan MJ, Dhruv HD, et al. Dependency of a therapy-resistant state of cancer cells on a lipid peroxidase pathway. Nature 2017;547(7664):453–457.
19. Yang WS, SriRamaratnam R, Welsch ME, et al. Regulation of ferroptotic cancer cell death by GPX4. Cell 2014; 156:317–331.
20. Kagan VE, Mao G, Qu F, et al. Oxidized arachidonic and adrenic PEs navigate cells to ferroptosis. Nat Chem Biol 2017;13:81–90.
21. Mayr L, Grabherr F, Schwärzler J, et al. Dietary lipids fuel GPX4-restricted enteritis resembling Crohn's disease. Nat Commun 2020;11:1775.
22. Hotamisligil GS. Inflammation, metaflammation and immunometabolic disorders. Nature 2017;542:177–185.
23. Lee YS, Wollam J, Olefsky JM. An integrated view of immunometabolism. Cell 2018;172:22–40.
24. Ozcan U, Cao Q, Yilmaz E, et al. Endoplasmic reticulum stress links obesity, insulin action, and type 2 diabetes. Science 2004;306:457–461.
25. Walter P, Ron D. The unfolded protein response: from stress pathway to homeostatic regulation. Science 2011; 334:1081–1086.
26. Hotamisligil GS. Endoplasmic reticulum stress and the inflammatory basis of metabolic disease. Cell 2010; 140:900–917.
27. Huang S, Xing Y, Liu Y. Emerging roles for the ER stress sensor IRE1α in metabolic regulation and disease. J Biol Chem 2019;294:18726–18741.
28. Grootjans J, Kaser A, Kaufman RJ, et al. The unfolded protein response in immunity and inflammation. Nat Rev Immunol 2016;16:469–484.
29. Kaser A, Lee AH, Franke A, et al. XBP1 links ER stress to intestinal inflammation and confers genetic risk for human inflammatory bowel disease. Cell 2008; 134:743–756.
30. Tschurtschenthaler M, Adolph TE, Ashcroft JW, et al. Defective ATG16L1-mediated removal of IRE1α drives Crohn's disease–like ileitis. J Exp Med 2017; 214:401–422.
31. Cao SS, Zimmermann EM, Chuang BM, et al. The unfolded protein response and chemical chaperones reduce protein misfolding and colitis in mice. Gastroenterology 2013;144:989–1000.e6.
32. Urano F, Wang X, Bertolotti A, et al. Coupling of stress in the ER to activation of JNK protein kinases by transmembrane protein kinase IRE1. Science 2000; 287:664–666.
33. Bennett BL, Sasaki DT, Murray BW, et al. SP600125, an anthrapyrazolone inhibitor of Jun N-terminal kinase. Proc Natl Acad Sci U S A 2001;98:13681–13686.
34. Wieser V, Adolph TE, Enrich B, et al. Reversal of murine alcoholic steatohepatitis by pepducin-based functional

blockade of interleukin-8 receptors. Gut 2017; 66:930–938.
35. Ingold I, Berndt C, Schmitt S, et al. Selenium utilization by GPX4 is required to prevent hydroperoxide-induced ferroptosis. Cell 2018;172. 409–22.e21.
36. Stewart CR, Stuart LM, Wilkinson K, et al. CD36 ligands promote sterile inflammation through assembly of a Toll-like receptor 4 and 6 heterodimer. Nat Immunol 2010; 11:155–161.
37. Keestra-Gounder AM, Byndloss MX, Seyffert N, et al. NOD1 and NOD2 signalling links ER stress with inflammation. Nature 2016;532:394–397.
38. Takeuchi O, Akira S. Pattern recognition receptors and inflammation. Cell 2010;140:805–820.
39. Miyamoto J, Igarashi M, Watanabe K, et al. Gut microbiota confers host resistance to obesity by metabolizing dietary polyunsaturated fatty acids. Nat Commun 2019;10:4007.
40. Yatsunenko T, Rey FE, Manary MJ, et al. Human gut microbiome viewed across age and geography. Nature 2012;486:222–227.
41. Turnbaugh PJ, Backhed F, Fulton L, et al. Diet-induced obesity is linked to marked but reversible alterations in the mouse distal gut microbiome. Cell Host Microbe 2008;3:213–223.
42. Kiechl S, Pechlaner R, Willeit P, et al. Higher spermidine intake is linked to lower mortality: a prospective population-based study. Am J Clin Nutr 2018; 108:371–380.
43. Imhann F, Van der Velde KJ, Barbieri R, et al. The 1000IBD project: multi-omics data of 1000 inflammatory bowel disease patients; data release 1. BMC Gastroenterol 2019;19:5.
44. Holen T, Norheim F, Gundersen TE, et al. Biomarkers for nutrient intake with focus on alternative sampling techniques. Genes Nutr 2016;11:12.
45. Wan Y, Wang F, Yuan J, et al. Effects of dietary fat on gut microbiota and faecal metabolites, and their relationship with cardiometabolic risk factors: a 6-month randomised controlled-feeding trial. Gut 2019;68:1417–1429.
46. Jostins L, Ripke S, Weersma RK, et al. Host-microbe interactions have shaped the genetic architecture of inflammatory bowel disease. Nature 2012;491:119–124.
47. Gorard DA, Hunt JB, Payne-James JJ, et al. Initial response and subsequent course of Crohn's disease treated with elemental diet or prednisolone. Gut 1993; 34:1198–1202.
48. di Caro S, Fragkos KC, Keetarut K, et al. Enteral nutrition in adult Crohn's disease: toward a paradigm shift. Nutrients 2019;11:2222.
49. Middleton SJ, Rucker JT, Kirby GA, et al. Long-chain triglycerides reduce the efficacy of enteral feeds in patients with active Crohn's disease. Clin Nutr 1995; 14:229–236.
50. Gunasekeera V, Mendall MA, Chan D, et al. Treatment of Crohn's disease with an IgG4-guided exclusion diet: a randomized controlled trial. Dig Dis Sci 2016; 61:1148–1157.
51. Torres J, Bonovas S, Doherty G, et al. ECCO guidelines on therapeutics in Crohn's disease: medical treatment. J Crohns Colitis 2020;14:4–22.
52. Levine A, Wine E, Assa A, et al. Crohn's disease exclusion diet plus partial enteral nutrition induces sustained remission in a randomized controlled trial. Gastroenterology 2019;157. 440–50.e8.
53. Ko CW, Qu J, Black DD, et al. Regulation of intestinal lipid metabolism: current concepts and relevance to disease. Nat Rev Gastroenterol Hepatol 2020;17:169–183.
54. Seiler A, Schneider M, Forster H, et al. Glutathione peroxidase 4 senses and translates oxidative stress into 12/15-lipoxygenase dependent- and AIF-mediated cell death. Cell Metab 2008;8:237–248.
55. Sengupta A, Lichti UF, Carlson BA, et al. Targeted disruption of glutathione peroxidase 4 in mouse skin epithelial cells impairs postnatal hair follicle morphogenesis that is partially rescued through inhibition of COX-2. J Invest Dermatol 2013;133:1731–1741.
56. Randolph GJ, Bala S, Rahier JF, et al. Lymphoid aggregates remodel lymphatic collecting vessels that serve mesenteric lymph nodes in Crohn disease. Am J Pathol 2016;186:3066–3073.
57. Adolph TE, Tomczak MF, Niederreiter L, et al. Paneth cells as a site of origin for intestinal inflammation. Nature 2013;503:272–276.
58. Kirkpatrick SI, Collins CE, Keogh RH, et al. Assessing dietary outcomes in intervention studies: pitfalls, strategies, and research needs. Nutrients 2018;10.
59. Jukic A, Bakiri L, Wagner EF, et al. Calprotectin: from biomarker to biological function. Gut 2021;70:1978–1988.
60. Belluzzi A, Brignola C, Campieri M, et al. Effect of an enteric-coated fish-oil preparation on relapses in Crohn's disease. N Engl J Med 1996;334:1557–1560.

Received May 13, 2021. Accepted January 4, 2022.

Correspondence
Address correspondence to: Timon E. Adolph, MD, PhD, Department of Internal Medicine I, Gastroenterology, Hepatology, Endocrinology & Metabolism, Medical University of Innsbruck, 6020 Innsbruck, Austria. e-mail: timon-erik.adolph@i-med.ac.at.

CRedit Authorship Contributions
Julian Schwärzler, MD (Conceptualization: Equal; Data curation: Lead; Formal analysis: Lead; Investigation: Lead; Methodology: Lead; Project administration: Lead; Visualization: Lead; Writing – original draft: Equal); Lisa Mayr, PhD (Conceptualization: Lead; Data curation: Lead; Formal analysis: Lead; Funding acquisition: Equal; Investigation: Lead; Methodology: Lead; Resources: Lead; Writing – original draft: Lead); Arnau Vich Vila, PhD (Conceptualization: Lead; Data curation: Lead; Formal analysis: Lead; Investigation: Lead; Methodology: Lead; Resources: Lead; Writing – original draft: Lead); Felix Grabherr, MD, PhD (Conceptualization: Equal; Data curation: Equal; Investigation: Equal; Writing – review & editing: Equal); Lukas Niederreiter, MD, PhD (Data curation: Equal; Methodology: Equal; Project administration: Equal; Writing – review & editing: Equal); Maureen Philipp, MD (Data curation: Equal; Formal analysis: Equal; Writing – review & editing: Equal); Christoph Grander, MD, PhD (Data curation: Supporting; Methodology: Supporting; Writing – review & editing: Supporting); Moritz Meyer, MD (Data curation: Supporting; Methodology: Supporting); Almina Jukic, MD (Data curation: Supporting; Methodology: Supporting); Simone Tröger, MD (Data curation: Equal; Formal analysis: Equal; Writing – review & editing: Equal); Barbara Enrich, BSc (Data curation: Equal; Formal analysis: Equal); Nicole Przysiecki, MSc (Data curation: Equal; Formal analysis: Equal); Markus Tschurtschenthaler, PhD (Methodology: Supporting); Felix Sommer, PhD (Data curation: Equal; Formal analysis: Equal; Writing – review & editing: Equal); Irmgard Kronberger, MD (Resources: Equal); Jakob Koch, MSc (Data curation: Equal; Formal analysis: Equal; Methodology: Equal); Richard Hilbe, BSc (Methodology: Equal; Resources: Equal; Writing – review & editing: Equal); Michael W. Hess, Dr. (Methodology: Equal; Writing – review & editing: Equal); Georg Oberhuber, Prof. (Formal analysis: Equal; Methodology: Equal); Susanne Sprung, MD (Formal analysis: Equal; Methodology: Equal); Qitao Ran, Prof. (Resources: Equal); Robert Koch, MD (Resources: Equal); Maria

Effenberger, MD (Resources: Equal); Nicole C. Kaneider, Dr. (Resources: Equal); Verena Wieser, MD, PhD (Data curation: Equal; Formal analysis: Equal); Markus A. Keller, Dr. (Data curation: Equal; Formal analysis: Equal); Rinse K. Weersma, MD, PhD (Funding acquisition: Equal; Methodology: Equal; Project administration: Equal; Resources: Equal; Writing – review & editing: Equal); Konrad Aden, MD (Writing – review & editing: Equal); Philip Rosenstiel, Prof. (Funding acquisition: Equal; Resources: Equal; Writing – review & editing: Equal); Richard S. Blumberg, MD, Prof. (Resources: Equal; Writing – review & editing: Equal); Arthur Kaser, MD, Prof. (Resources: Equal; Writing – review & editing: Equal); Herbert Tilg, MD, Prof. (Funding acquisition: Equal; Resources: Equal; Supervision: Equal; Writing – review & editing: Equal); Timon Erik Adolph, MD, PhD (Conceptualization: Lead; Funding acquisition: Lead; Project administration: Lead; Supervision: Lead; Validation: Lead; Writing – original draft: Lead).

Conflicts of interest
The authors declare no conflicts.

Funding
T.E.A. is grateful for the support from the European Research Council (#101039320). This study was supported by the Austrian Science Fund (FWF P33070) and the European Crohn's and Colitis Organisation (to TEA), the Excellence Initiative (Competence Centers for Excellent Technologies) of the Austrian Research Promotion Agency FFG: Research Center of Excellence in Vascular Ageing Tyrol, VASCage (K-Project no. 843536; funded by BMVIT, BMWFW, Wirtschaftsagentur Wien and Standortagentur Tirol; to HT), the Austrian Society of Gastroenterology and Hepatology (to LM), the German Funding Agency through SO1141/10-1 (to FS), Research Unit FOR5042 (P3 and P5 to FS and PR), CRC1182 (C2 to FS and PR), IMI2 grant ImmUniverse and EXC2167 (to PR), CRC1371 (project ID 395357507, P11 to MT), and BMBF under the grant approval no. 01ZX1915A (to KA), the Seerave Foundation, the TIMID project (LSHM18057-SGF; financed by the PPP allowance made available by Top Sector Life Sciences and Health to Samenwerkende Gezondheidsfondsen [SGF] to stimulate public- private partnerships and co-financing by health foundations that are part of the SGF, and an unrestricted research grant from Takeda Pharmaceuticals; to RSW), the National Institutes of Health (NIH NIDDK R01DK088199 to RSB), the intramural funding program of the Medical University of Innsbruck for young scientists MUI-START (Project 2020-01-017 to LN), and the Tiroler Wissenschaftsförderung (to LN and FG).